Biosensors and Bioelectronics 24 (2009) 2991–2996

Contents lists available at ScienceDirect

Biosensors and Bioelectronics

journal homepage: www.elsevier.com/locate/bios

A nitrite biosensor based on the immobilization of Cytochrome *c* on multi-walled carbon nanotubes–PAMAM–chitosan nanocomposite modified glass carbon electrode

Quanpeng Chen[b], Shiyun Ai[a,*], Xiangbin Zhu[b], Huanshun Yin[a], Qiang Ma[a], Yanyan Qiu[a]

[a] College of Chemistry and Material Science, Shandong Agricultural University, Taian 271018, Shangdong, PR China
[b] College of Resources and Environment, Shandong Agricultural University, Taian 271018, Shandong, PR China

ARTICLE INFO

Article history:
Received 5 January 2009
Received in revised form 1 March 2009
Accepted 4 March 2009
Available online 17 March 2009

Keywords:
Nitrite biosensor
Cytochrome *c*
Nitrite
MWNT–PAMAM–Chit nanocomposite

ABSTRACT

A novel nitrite biosensor was successfully prepared via immobilizing Cytochrome *c* (Cyt *c*) onto the multi-walled carbon nanotubes–poly(amidoamine) (PAMAM)–chitosan (MWNT–PAMAM–Chit) nanocomposite modified glass carbon electrode (GCE). Ultraviolet and visible (UV–vis) absorption spectrum, cyclic voltammetry (CV) and electrochemical impedance spectroscopy (EIS) were used to examine the native conformation and bioactivity of the immobilized Cyt *c*, and the electrochemical properties of the modified electrodes, respectively. The results indicate that the immobilized Cyt *c* retained its native characters, and the MWNT–PAMAM–Chit nanocomposite is a good platform for the immobilization of Cyt *c* as well as an excellent promoter for the electron transfer between Cyt *c* and electrode. The high reactive Cyt *c* π-cation, which can oxidize NO_2^- into NO_3^- in the solution, is generated at higher potential (>0.7 V) based on the further oxidation of Cyt *c*. The nitrite biosensor showed a fast response to nitrite (about 5 s) in two concentration intervals, one was from 0.1 to 29 μM, and the other from 29 to 254 μM. The low detection limit of 0.01 μM was obtained.

1. Introduction

The development of catalytic electrode materials for the determination of nitrite is receiving considerable attention due to the potential toxicity of its anion, which can easily interact with amines to form toxic and carcinogenic nitrosoamines (Konstantinou et al., 2006; Vishnuvardhan et al., 2008). Many methods for nitrite determination have been developed (Moorcroft et al., 2001), such as spectroscopic analysis, capillary electrophoresis, polarographic analysis and chromatography, etc. However, it must be pointed out that these centralized and sophisticated analytical systems need complicated process and expensive instruments. Owing to the rapid response, high sensitivity, low-cost, time-saving and simple use, much attention has been paid to the development of high-performance nitrite sensors (Cao and Wang, 2009; Huang et al., 2008), especially biosensors (Dai et al., 2008; Zhao et al., 2006; Almeida et al., 2007; Yang et al., 2005; Wu et al., 1997). Most nitrite biosensors were attributed to the catalysis of proteins for the reductive reaction of nitrite. But few investigations for electrochemical oxidation of nitrite were reported due to the required undesirable high overvoltages. Recently, the first nitrite biosensor based on Cytochrome *c* (Cyt *c*) was fabricated which showed excellent biocatalytic oxidative property to nitrite (Geng et al., 2008). This study opened up a new prospect for the determination of nitrite, at the same time, a new field for the application of Cyt *c*.

Cyt *c*, a pseudo-spherical basic redox protein with relatively small size (2.6 nm × 3.2 nm × 3.0 nm), plays an important role in the biological respiratory chain, whose function is to transfer electrons between membrane-bound enzyme complexes of Cyt *c* reductase and Cyt *c* oxidase (Hartmann, 2005; Oellerich et al., 2002; Ochiai, 1997). It is well known that Cyt *c* has the ability to electrocatalyze the reduction of hydrogen peroxide (H_2O_2). But more and more studies have discovered its potential application for the detection of other substances, such as nitric oxide (Koh et al., 2008), superoxide radical anion (Ding et al., 2007), halogen oxyanions, ascorbic acid (AA) and L-cysteine (LC) (Shie et al., 2008), indicating that the search for further application of Cyt *c* is still of considerable interest. As a relatively simple metalloprotein, Cyt *c* is an ideal model for studying biological electron transfer processes (Moore and Pettigrew, 1990). However, it is difficult for Cyt *c* to undergo a facile redox process at conventional electrodes. The important reason is that not only electroactive center was deeply buried, but also both electrochemical activity and bioactivity would be denatured and damaged when the protein adsorbed on the electrode surface (Lin et al., 2008). The first promoter, 4,4′-bipyridyl, for the electrochemical study of Cyt *c* at a gold electrode was reported in 1977 (Eddowes and Hill,

* Corresponding author. Tel.: +86 538 8247660; fax: +86 538 8242251.
E-mail address: ashy@sdau.edu.cn (S. Ai).

0956-5663/$ – see front matter © 2009 Elsevier B.V. All rights reserved.
doi:10.1016/j.bios.2009.03.007

1977). Since then, many other compounds were found to be seized of the promoter action such as sulfur bridged bipyridines (Taniguchi et al., 1982), bis(4-pyridyl)disulfide and purine (Taniguchi et al., 1984). Recently, a mass of studies have been reported in order to improve the direct electron transfer between Cyt *c* and electrode mainly based on the modification of electrodes with various electron transfer mediators. The modification of electrodes with Cyt *c* basically followed two strategies: (i) electrostatic adherence, such as the modified electrodes reported in the references (Zhu et al., 2008; Ji et al., 2006; Shie et al., 2008; Koh et al., 2008; Xiang et al., 2008; Dai et al., 2004); (ii) covalent bond, such as those in (Zhou et al., 2008; Zhang, 2008; Zhang et al., 2009; Ding et al., 2007; Chen et al., 2008).

Among various dendrimers, poly(amidoamine) (PAMAM) dendrimers have received a great deal of attention due to its quite open spherical 3D structures at high generation and good biocompatibility (Shen and Hu, 2005). The amino groups with high density in PAMAM are easily functionalized by other substances, greatly extending their applications. Up to now, PAMAM dendrimers have been successfully applied in the fabrication of biosensors such as DNA electrochemical biosensor (Shi et al., 2008) and amperometric glutamate biosensor (Tang et al., 2007). More attractively, novel multi-walled carbon nanotubes (MWNT) nanocomposite, synthesized by grafting G4 PAMAM dendrimers on carboxylated carbon nanotubes, was reported for glucose detection based on the immobilization of glucose oxidase (GO_x) and horseradish peroxidase (HRP) (Zeng et al., 2007). This biosensor exhibited very high sensitivity and fast response to glucose, indicating that the further research for the combination of PAMAM dendrimers and MWNT is of great significance.

In this study, G4 PAMAM dendrimers and MWNT were dispersed in chitosan (Chit) solution to form the resulting MWNT–PAMAM–Chit nanocomposite, which was used as the substrate to immobilize Cyt *c* on glass carbon electrode (GCE) with GA acting as the coupling agent. The redox behavior of Cyt *c* and the electrochemical response of the modified electrode to nitrite were researched. To our best knowledge, there are no published data for the application of MWNT–PAMAM–Chit nanocomposite in the immobilization of Cyt *c* as well as the fabrication of the nitrite biosensor.

2. Experimental

2.1. Reagents

Horse heart Cytochrome *c* (MW 12384) was purchased from Sigma and used without further purification. 1 mM Cyt *c* stock solution was prepared by 0.1 M pH 7.0 phosphate buffer solution (PBS), and stored at a temperature of 4 °C. Chitosan was obtained from Aldrich and used as received. A 0.2 wt.% chitosan solution was prepared by dissolving chitosan in 1 wt.% acetic acid solution. PAMAM dendrimers were synthesized according to the reported procedure (Tomalia et al., 1985, 1986). A methanol solution of 20% G4 PAMAM dendrimers was purified by dialyzing. MWNT were purchased from Nachen S&T Ltd. (Beijing, China) and treated according to reported procedure (Zeng et al., 2007; Furtado et al., 2004). All other materials were of at least analytical grade and used as received without further purification. 0.1 M PBS was prepared by mixing the stock solutions of Na_2HPO_4 and NaH_2PO_4. Doubly distilled and deionized water was used through this work.

2.2. Preparation of the modified electrodes

Before modification, the bare GCE (from CH Instruments, Shanghai, China; diameter: 0.004 m; the type of glassy carbon is type II of Europe) was polished to a mirror-like surface with 0.05 μm Al_2O_3 slurry, then rinsed with water, ultrasonicated in 1:1 (v/v) HNO_3, ethanol and doubly distilled water, respectively. Finally, it was dried under the stream of high purity nitrogen for further use. The calculated amount MWNT and 5 μl solution of 20% PAMAM dendrimers in methanol were homogeneously dispersed in 1 ml 0.2 wt.% chitosan solution at room temperature with the aid of ultrasonic agitation. Then 7.5 μl of the resulting mixture was dropped onto the cleaned GCE surface to prepare MWNT–PAMAM–Chit/GCE. To immobilize Cyt *c* onto the electrode, 5 μl 20% GA solution was first spread onto the resulting MWNT–PAMAM–Chit/GCE surface and exposed to the air for 2 h at room temperature, and then rinsed with the double distilled water to remove any physically adsorbed GA and dried in the air at room temperature (noted GA/MWNT–PAMAM–Chit/GCE). Finally, 7.5 μl of 0.1 mM solution of Cyt *c* in 0.1 M pH 7.0 PBS was dropped onto the surface of GA/MWNT–PAMAM–Chit/GCE and reacted for 2 h. The electrode referred in the text as Cyt *c*/GA/MWNT–PAMAM–Chit/GCE was obtained and preserved in a refrigerator at 4 °C after being washed with 0.1 mM PBS solution.

2.3. UV–vis and electrochemical measurements

Ultraviolet and visible (UV–vis) absorption spectrum was obtained using Shimazu 5301 UV-spectrophotometer at room temperature. All the electrochemical experiments were performed by using a CHI 660C electrochemical workstation (CH Instruments, Shanghai, China). A conventional three-electrode system was used in the measurements with a saturated calomel electrode (SCE) as the reference, a Pt wire as the auxiliary electrode and a bare or a modified electrode as the working electrode. Electrochemical impedance spectroscopy (EIS) was performed in 0.1 M KCl solution within the frequency range of 10^{-2} to 10^5 Hz with 5.0 mM $K_3Fe(CN)_6/K_4Fe(CN)_6$ (1:1) mixture as electroactive probe. Cyclic voltammetry (CV) was conducted in 0.1 M pH 7.0 PBS containing $NaNO_2$ with different concentrations. Prior to measurement, electrolytic solutions were purged with highly purified nitrogen for at least 10 min, and then a nitrogen atmosphere was maintained over the electrochemical cell during the experiments. All experiments were carried out at room temperature.

3. Results and discussion

3.1. UV–vis absorption spectroscopic characterization

The UV–vis spectrum was used to determine whether the immobilized Cyt *c* denatured or not. Cyt *c* aqueous solution gave a heme band at 410 nm in 0.1 M pH 7.0 PBS as shown in Fig. 1a. There were no absorption bands on MWNT–PAMAM–Chit nanocomposite as seen from Fig. 1b. When Cyt *c* was immobilized on MWNT–PAMAM–Chit nanocomposite (Fig. 1c, which was recorded by directly casting MWNT–PAMAM–Chit nanocomposite, 20% glutaraldehyde solution and Cyt *c* solution onto a glass sheet sequentially), a slight absorption band was observed at the same position to that of Cyt *c* solution, indicating that the immobilized Cyt *c* maintained its native structure and retained its native conformation and bioactivity (Rusling, 1998). The weak absorption peak could be attributed to the small quantity of the immobilized Cyt *c*.

3.2. Electrochemical impedance spectroscopy

EIS is a high effective method for probing the features of surface-modified electrodes. In this study, EIS was carried out to investigate the changes of electron transfer resistance (Ret) that aroused from every surface modification step as shown in Fig. 2. The bare GCE (Fig. 2a) manifested as a simple electron transfer reaction's Nyquist

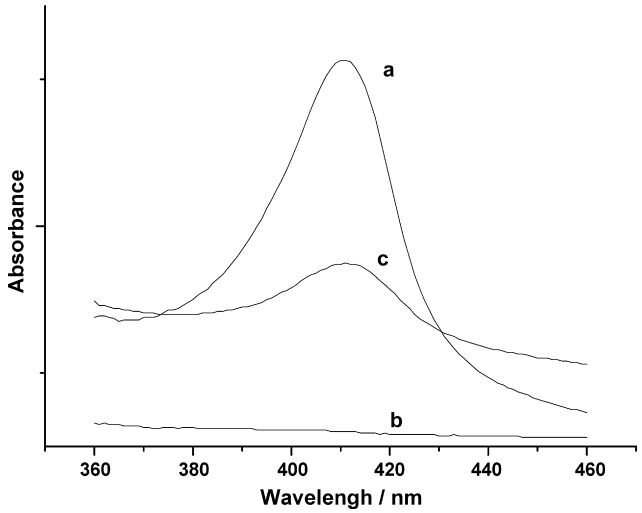

Fig. 1. The UV–vis absorption spectra for (a) Cyt *c* in 0.1 M pH 7.0 PBS, (b) MWNT–PAMAM–Chit nanocomposite, (c) Cyt *c* immobilized on MWNT–PAMAM–Chit nanocomposite.

plot. It exhibited an almost straight line at low frequencies corresponding to the diffusion process, and a very small semicircle at high frequencies. Ret could be estimated about 600 Ω from the diameter. After coated with PAMAM–Chit (Fig. 2b), the EIS showed an almost straight line at all frequencies which suggested that the electrode reaction was controlled by diffusion. This revulsion could be attributed to the electrostatic interaction between $(Fe(CN)_6)^{3-/4-}$ and amino groups of PAMAM dendrimers on the surface of modified electrode. The same result was also observed at MWNT–PAMAM–Chit/GCE (Fig. 2c), indicating that the doped MWNT did not fundamentally change the surface characteristics of the electrode. From Fig. 2d it is apparent that the Ret increased dramatically to about 3000 Ω, which proved the higher steric hindrance – ferri/ferrocyanide ions could not approach to the electrode surface after binding of glutaraldehyde. However, obvious decrease of interfacial resistance (Ret ≈ 800 Ω) is observed in Fig. 2e, which indicates the successful immobilization of Cyt *c* on the modified electrode surface. Because the bonding between negatively charged aldehyde groups and positively charged lysine residue of Cyt *c* offered an easy access for the ferri/ferrocyanide ions in PBS to the

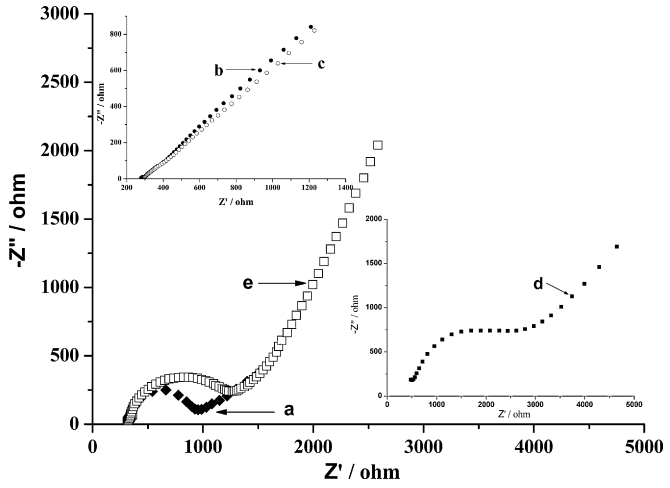

Fig. 2. Nyquist plots of EIS in 0.1 M KCl solution containing 5.0 mM $K_3(Fe(CN)_6)/K_4(Fe(CN)_6)$ (1:1) for bare GCE (a), PAMAM–Chit/GCE (b), MWNT–PAMAM–Chit/GCE (c), GA/MWNT–PAMAM–Chit/GCE (d), Cyt *c*/GA/MWNT–PAMAM–Chit/GCE (e). The amplitude: 0.005; the potential: 0.169 V.

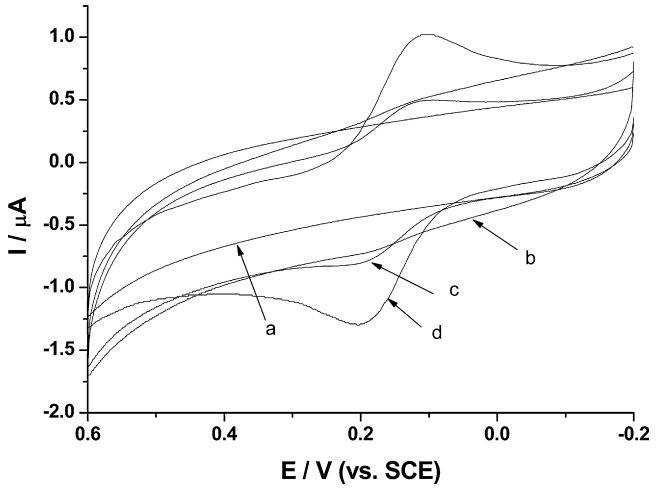

Fig. 3. CVs of Cyt *c*/GA/GCE (a), Cyt *c*/GA/Chit/GCE (b), Cyt *c*/GA/PAMAM–Chit/GCE (c) and Cyt *c*/GA/MWNT–PAMAM–Chit/GCE (d) in 0.1 M pH 7.0 PBS at 0.05 V s^{-1}.

attached Cyt *c*. It is in close accord with the previous reports (Zhao et al., 2005; Wang et al., 2002a).

3.3. Cyclic voltammetric behaviors of the immobilized Cyt c

The cyclic voltammetry was performed to investigate the influences of Chit, PAMAM dendrimers and MWNT on the direct electrochemistry of Cyt *c*, respectively. Fig. 3 shows the cyclic voltammetric behaviors of different modified electrodes in 0.1 M pH 7.0 PBS at 0.05 V s^{-1}. Neither Cyt *c*/GA/GCE (Fig. 3a) nor Cyt *c*/GA/Chit/GCE (Fig. 3b) appeared any peaks, but a slight oxidation–reduction was observed on Cyt *c*/GA/PAMAM–Chit/GCE (Fig. 3c). This result clearly demonstrated that PAMAM dendrimers successfully acted as a substrate for the immobilization of Cyt *c* on the surface of glass carbon electrode and facilitated the electron exchange between the Cyt *c* and the electrode. In addition, it must be pointed out that GA, served as the coupling agent in the process of immobilization of Cyt *c*, could react with the amino groups of PAMAM dendrimers on the electrode surface and the lysine residue of Cyt *c* (p*I* 10), respectively. The amount of amino groups on the surface of PAMAM–Chit/GCE was much more than that of the bare GCE and Chit/GCE. In other words, PAMAM–Chit/GCE would provide more binding sites for reacting with GA and finally leading to the increase of the fixation chamber of Cyt *c* on the electrode surface.

The subtle electronic properties suggested that carbon nanotubes had the ability to promote electron transfer reactions when used as an electrode material in electrochemical reactions (Wang et al., 2002b). In our work, this notable promotion was also confirmed. Upon comparison of Fig. 3c and d, the modified electrode involving MWNT, Cyt *c*/GA/MWNT–PAMAM–Chit/GCE, exhibited a couple of stable redox peaks at 0.203 V (anodic peak) and 0.104 V (cathodic peak), which was 2.5 times larger than that of Cyt *c*/GA/PAMAM–Chit/GCE.

The influence of the amount of doped MWNT on the electrochemical property of the immobilized Cyt *c* was further investigated, and the data are listed in Table 1. As we can see from Table 1, both the anodic and cathodic peak currents firstly increased with the increasing doped amount of MWNT, and then decreased remarkably after doping 0.125 mg ml^{-1}. Hence, 0.125 mg ml^{-1} was chosen as the optimal doping amount. Such phenomena may be noted that MWNT with low concentration (≤0.125 mg ml^{-1}) mainly play a catalytic role in the electrode reaction based on its essential characteristics, but with high concentration (>0.125 mg ml^{-1}), the increased amount of carboxy groups involved in MWNT–PAMAM–Chit nanocomposite make high space

Table 1
The influence of the amount of doped MWNT on the direct electrochemistry of immobilized Cyt *c*.

MWNT (mg ml^{-1})	Midpoint potential, $E_{1/2}$ (vs. SCE) (V)	I_{pa} (μA)	I_{pc} (μA)
0.000	0.143	−0.24	0.23
0.050	0.164	−0.36	0.32
0.100	0.168	−0.83	0.71
0.125	0.154	−1.25	1.20
0.150	0.159	−0.85	0.76
0.200	0.164	−0.46	0.42
0.300	–	–	0.33

steric hindrance between amino group and GA on the surface of modified electrode, finally leading to a less fixation chamber of Cyt *c* on the modified electrode. As a result, a decreased peak current was observed.

The midpoint potential $E_{1/2}$ (vs. SCE) of immobilized Cyt *c*, 0.154 V, is more positive than that of native Cyt *c* (0.046 V). It may be noted that the reversible electron exchange could occur with monomeric Cyt *c* layer on the surface of modified GCE. In this situation, the apparent reversibility decreased since the surface was partially covered with polymeric species which could only be oxidized at higher potentials (Wael et al., 2008).

The pH effect of supporting electrolyte on the formal potential of the immobilized Cyt *c* was also investigated (not shown). Nearly reversible voltammograms with stable and well-defined redox peaks were obtained in the pH range of 5.0–8.0. The formal potential shifted negatively along with the increase of pH. A linear relationship was obtained between the formal potential and pH with the slope of 15.1 mV pH^{-1}, suggesting that the electrochemistry of Cyt *c* involved a proton process (Geng et al., 2008). This slope is much smaller than the theoretical value (59 mV pH^{-1}) for the electrons transfer accompanied with an equal number of protons in electrode reaction, which could be attributed to the influence of the protonation states of trans ligands to the heme iron and amino acids around Cyt *c*, or the protonation of the water molecule coordinated to the central iron (Yamazaki et al., 1978).

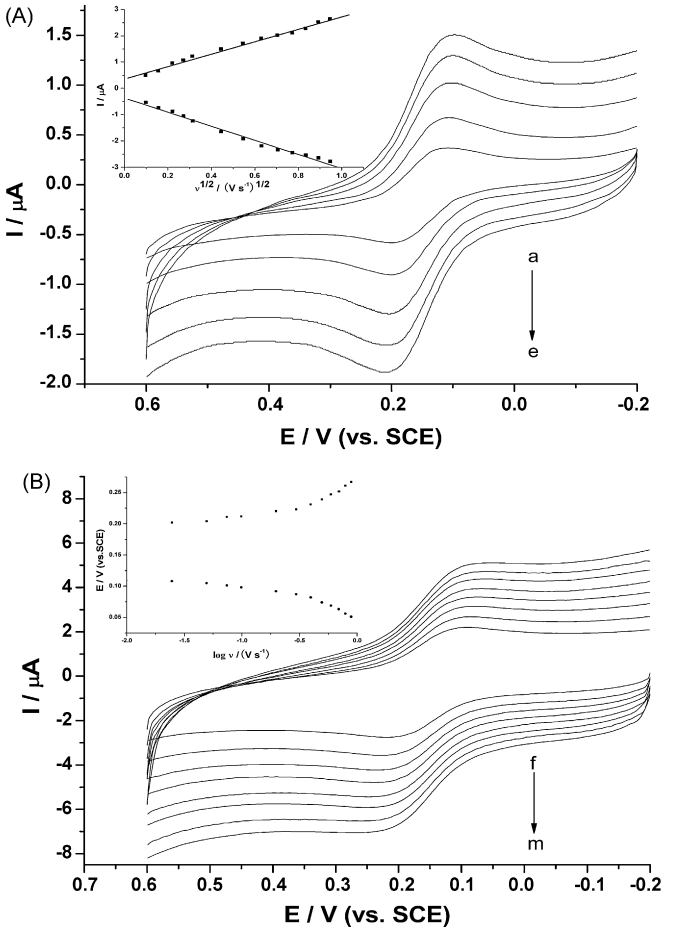

Fig. 4. (A) and (B) CVs of Cyt *c*/GA/MWNT–PAMAM–Chit/GCE at different scan rates in 0.1 M pH 7.0 PBS. Scan rates from (a) to (m) are 0.01, 0.025, 0.05, 0.075, 0.1, 0.2, 0.3, 0.4, 0.5, 0.6, 0.7, 0.8, 0.9 V s^{-1}, respectively. Insert of (A): plots of anodic and cathodic peak currents vs. the square root of scan rate. Insert of (B): variation of anodic and cathodic peak potentials vs. the logarithm of scan rate.

3.4. Influence of scan rate

Fig. 4 shows CVs for Cyt *c*/GA/MWNT–PAMAM–Chit/GCE in 0.1 M pH 7.0 PBS at different scan rate. The cathodic and anodic peak currents linearly increased with the square root of the scan rate ($\upsilon^{1/2}$) from 0.01 to 0.9 V s^{-1} (shown in insert of Fig. 4A). In other words, the current function ($i_p/\upsilon^{1/2}$) had a constant value at different scan rates, indicating that the electrode reaction of Cyt *c* immobilized on the modified electrode was mainly controlled by a diffusion control process.

With increasing of scan rate, the oxidation peak shifted to more positive potentials, while the reduction peak shifted to more negative potentials. As shown in insert of Fig. 4B, two linear relationships were observed when $\upsilon > 0.3$ V s^{-1}, by plotting E_p vs. logυ. On the basis of Laviron's method (Laviron, 1979): A graph of $E_p = f(\log \upsilon)$ yields two straight lines with a slope equal to $-2.3RT/\alpha nF$ for the cathodic peak, and $2.3RT/(1-\alpha)nF$ for the anodic peak, the charge transfer coefficient, α, was estimated to be 0.53. The average electron transfer rate constant, $k_s = 2.4$ s^{-1}, can be obtained according to Eq. (1). This k_s value is much higher than that of the first nitrite biosensor based on Cyt *c* (1.39 s^{-1}) (Geng et al., 2008) and other Cyt *c* modified electrodes such as Cyt *c*/poly-TTCA modified electrode (1.86 s^{-1}) (Koh et al., 2008) and Cyt *c*/NaY/GCE (0.78 ± 0.04 s^{-1}) (Dai et al., 2004), indicating that the MWNT–PAMAM–Chit nanocomposite acted as a good platform for the immobilization of Cyt *c*, at the same time, an excellent promoter for the electron transfer between Cyt *c* and the electrode.

$$\log k_s = \alpha \log(1-\alpha) + (1-\alpha)\log\alpha - \log\left(\frac{RT}{nF\upsilon}\right) - \frac{\alpha(1-\alpha)nF\Delta E_p}{2.3RT} \quad (1)$$

According to $Q = nFA\Gamma$, where Q is the charge involved in the reaction, n the number of electron transferred, F the Faraday's constant, and A the electrode area (herein, the geometric area of GCE is used). The surface coverage (Γ) of Cyt *c* immobilized on the surface of the modified electrode could be calculated to be 1.4×10^{-11} mol cm^{-2}, which is 10 times the theoretical monolayer coverage of 1.4×10^{-12} mol cm^{-2} (Dickerson et al., 1971). Because G4 PAMAM dendrimers are approximately spherical molecules with higher amino group densities, a three dimensional space will be established for the connection between the amino groups of PAMAM dendrimers and the lysine residue of Cyt *c* with the coupling agent of GA. As a result, the real area for the immobilization of Cyt *c* is much higher than that of the electrode geometric area for the estimation of surface coverage.

3.5. Biocatalytic oxidation of nitrite on Cyt c/GA/MWNT–PAMAM–Chit/GCE

The first oxidative nitrite biosensor based on Cyt *c* was reported recently and a possible mechanism-biocatalytic oxidative property

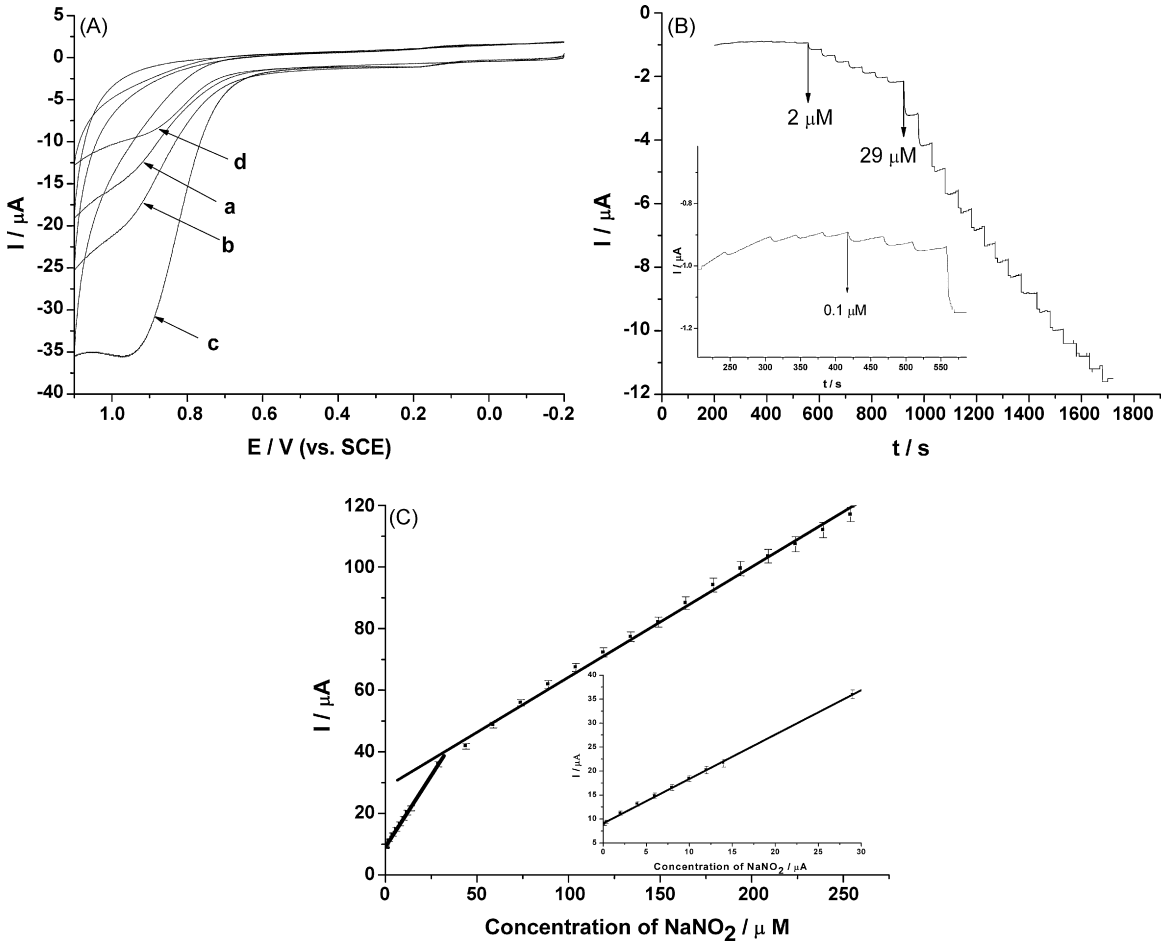

Fig. 5. (A) CVs of Cyt *c*/GA/MWNT–PAMAM–Chit/GCE in 0.1 M PBS containing 0 (a), 0.02 mM (b), 0.1 mM (c) $NaNO_2$, and the bare GCE in 0.1 M pH 7.0 PBS containing 0.1 mM $NaNO_2$ (d). Scan rate: 0.05 V s^{-1}. (B) Typical current–time curve of the Cyt *c*/GA/MWNT–PAMAM–Chit/GCE upon the successive addition of 0.3, 2 and 29 μM $NaNO_2$ into gently stirred 0.1 M pH 7.0 PBS. Applied potential: 0.9 V. (C) Linear relation between the amperometric response and $NaNO_2$ concentration.

to nitrite was proposed (Geng et al., 2008), which could be divided into three steps as shown in the following reactions:

$$Fe^{2+}\text{–Cyt } c \rightarrow Fe^{3+}\text{–Cyt } c + e^- \quad (2)$$

$$Fe^{3+}\text{–Cyt } c \rightarrow [Fe^{4+}\text{–Cyt } c]^{\bullet} + 2e^- \quad (3)$$

$$[Fe^{4+}\text{–Cyt } c]^{\bullet} + NO_2^- + H_2O \rightarrow Fe^{3+}\text{–Cyt } c \rightarrow + NO_3^- + 2H^+ \quad (4)$$

Firstly, ferrous Cyt *c* was oxidized to ferric form at low potential, and then the ferric Cyt *c* was further oxidized into $[Fe^{4+}$–Cyt $c]^{\bullet}$ at higher potential. $[Fe^{4+}$–Cyt $c]^{\bullet}$ is a highly reactive Cyt *c* π-cation which could oxidize NO_2^- into NO_3^- in the solution.

In this work, the oxidation of Cyt *c* and the biocatalytic oxidative property to nitrite were also investigated. Fig. 5A shows the result obtained from investigation of the CVs of Cyt *c*/GA/MWNT–PAMAM–Chit/GCE in 0.1 M pH 7.0 PBS containing different concentrations of $NaNO_2$. In the bulk PBS solution, two-step electrochemical oxidation of Cyt *c* corresponding to reactions (2) and (3) is observed in Fig. 5A(a). The further oxidation of Cyt *c* appeared when the potential increased to 0.7 V. When 0.02 mM $NaNO_2$ was added into the bulk solution (curve b, Fig. 5A), the anodic peak current at higher potential enhanced obviously. It could be herein attributed to the interaction between the highly reactive Cyt *c* π-cation and $NaNO_2$. Upon comparison of Fig. 5A(b) and (c), sharper peak current was observed at higher $NaNO_2$ concentration, indicating the high sensitivity of the biosensor to the difference of $NaNO_2$ concentration. Moreover, the peak current of 0.1 mM $NaNO_2$ at Cyt *c*/GA/MWNT–PAMAM–Chit/GCE (curve c, Fig. 5A) is about 20 times than that of the bare GCE (curve d, Fig. 5A), suggesting that the modified electrode mediates the oxidation of $NaNO_2$ greatly.

Fig. 5B shows the amperometric response of Cyt *c*/GA/MWNT–PAMAM–Chit/GCE at 0.9 V upon successive additions of different concentrations of $NaNO_2$. As $NaNO_2$ was added with regular speed into the gentle stirring PBS solution, the modified electrode could attain the steady state current within less than 5 s, which is a very rapidly response to the change of $NaNO_2$ concentration. The response was proportional to the concentration of $NaNO_2$ in the ranges of 0.1–29 μM ($r = 0.996$) and 29–254 μM ($r = 0.997$), as shown in Fig. 5C. The total range of the biosensor, 0.1–254 μM, was rough agreement with that of the first nitrite biosensor based on Cyt *c* (1–1000 μM), while the detection limit was estimated to be 0.01 μM at a signal-to-noise ratio of 3, which was obviously lower than that of the first one (0.5 μM) (Geng et al., 2008), indicating an extraordinary improvement in sensitivity of such nitrite biosensors. Furthermore, the detection limit was also lower than that of other nitrite sensors and biosensors such as MnO_2/QPOE composite electrodes (0.36 μM) (Cao and Wang, 2009), Hb/HS–CdS modified GCE (0.08 μM) (Dai et al., 2008) and Mb–ZnO-modified GE (4 μM) (Zhao et al., 2006), indicating that this proposed method could potentially be used for monitoring of the concentration of $NaNO_2$ sensitively. The lower detection limit could be ascribed to the high loading of Cyt *c* on the electrode surface via the present method and the rapid electron transfer between them.

Possible interference for the detection of nitrite on this biosensor was also investigated by addition of various ions, such as K^+, Na^+, Mg^{2+}, Ca^{2+}, Zn^{2+}, F^-, Cl^-, $NO_3{}^-$, $SO_4{}^{2-}$, $H_2PO_4{}^-$, $HPO_4{}^{2-}$ and $PO_4{}^{3-}$, into the PBS solution (pH 7.0) containing 10 μM $NaNO_2$. No interference was found with the determination in a 100-fold concentration, and in 50-fold amount of dopamine and L-tryptophane also.

The stability and reproducibility of Cyt *c*/GA/MWNT–PAMAM–Chit/GCE were analyzed. The peak currents of the modified electrode after continuous scanning of 50 cycles, in the blank solution over the potential range from −0.8 to +0.7 V, were consistent with the first scanning cycle. The standard deviation of the peak currents was only 4.6% comparing to 7 times modified electrodes with same treatment. The electrode still retained about 90% of its initial sensitivity for the oxidation of $NaNO_2$ after stored in 0.1 M pH 7.0 PBS at 4 °C for 30 days.

4. Conclusions

MWNT–PAMAM–Chit nanocomposite was first used as the substrate for the immobilization of Cyt *c* on GCE with the coupling agent of GA. The facts that MWNT–PAMAM–Chit nanocomposite provides a perfect platform for the immobilization of Cyt *c* and facilitates the electron exchange between the Cyt *c* and electrode can be obtained from the CV and EIS results. The immobilized Cyt *c* displayed a good electrocatalytic response to the oxidation of nitrite, which was attributed to the highly reactive Cyt *c* π-cation generated by the further oxidation of Cyt *c*. The obtained novel nitrite biosensor exhibited two wide linear ranges, low detection limit, good reproducibility and stability. This study provides an efficient strategy for the immobilization of Cyt *c* and plays a great role in promoting the construction of nitrite biosensors.

Acknowledgements

This work was supported by the National Natural Science Foundation of China (No. 20775044) and the Natural Science Foundation of Shandong province, China (Y2006B20).

References

Almeida, M.G., Silveira, C.M., Moura, J.J.G., 2007. Biosens. Bioelectron. 22, 2485–2492.
Cao, X., Wang, N., 2009. Sens. Actuators, B 137, 710–714.
Chen, X.J., West, A.C., Cropek, D.M., Banta, S., 2008. Anal. Chem. 80, 9622–9629.
Dai, Z., Bai, H., Hong, M., Zhu, Y., Bao, J., Shen, J., 2008. Biosens. Bioelectron. 23, 1869–1873.
Dai, Z., Liu, S., Ju, H., 2004. Electrochim. Acta 49, 2139–2144.
Dickerson, R.E., Takano, T., Eisenberg, D., Kallai, O.B., Samson, L., Cooper, A., Margoliash, E., 1971. J. Biol. Chem. 246, 1511–1535.
Ding, S., Wei, W., Zhao, G., 2007. Electrochem. Commun. 9, 2202–2206.
Eddowes, M.J., Hill, H.A.O., 1977. J. Chem. Soc. Chem. Commun. 21, 771–772.
Furtado, C.A., Kim, U.J., Gutierrez, H.R., Pan, L., Dickey, E.C., Eklund, P.C., 2004. J. Am. Chem. Soc. 126, 6095–6105.
Geng, R., Zhao, G., Liu, M., Li, M., 2008. Biomaterials 29, 2794–2801.
Hartmann, M., 2005. Chem. Mater. 17, 4577–4593.
Huang, X., Li, Y., Chen, Y., Wang, L., 2008. Sens. Actuators, B 134, 780–786.
Ji, X., Jin, B., Jin, J., Nakamura, T., 2006. J. Electroanal. Chem. 590, 173–180.
Koh, W.C.A., Rahman, M.A., Choe, E.S., Lee, D.K., Shim, Y.B., 2008. Biosens. Bioelectron. 23, 1374–1381.
Konstantinou, I.K., Hela, D.G., Albanis, T.A., 2006. Environ. Pollut. 141, 555–570.
Laviron, E., 1979. J. Electroanal. Chem. 101, 19–28.
Lin, L., Qiu, P., Cao, X., Jin, L., 2008. Electrochim. Acta 53, 5368–5372.
Moorcroft, M.J., Davis, J., Compton, R.G., 2001. Talanta 54, 785–803.
Moore, G.R., Pettigrew, G.W., 1990. Cytochromes c, Evolutionary, Structural and Physicochemical Aspects. Springer-Verlag, Berlin.
Ochiai, E., 1997. J. Chem. Educ. 74, 600–604.
Oellerich, S., Wackerbarth, H., Hildebrandt, P., 2002. J. Phys. Chem. B 106, 6566–6580.
Rusling, J.F., 1998. Acc. Chem. Res. 31, 363–369.
Shen, L., Hu, N., 2005. Biomacromolecules 6, 1475–1483.
Shi, W., Ai, S., Li, J., Zhu, L., 2008. Chin. J. Anal. Chem. 36, 335–338.
Shie, J., Yogeswaran, U., Chen, S., 2008. Talanta 74, 1659–1669.
Tang, L., Zhu, Y., Xu, L., Yang, X., Li, C., 2007. Talanta 73, 438–443.
Taniguchi, I., Iseki, M., Yamaguchi, H., Yasukouchi, K., 1984. J. Electroanal. Chem. 175, 341–348.
Taniguchi, I., Toyosawa, K., Yamaguchi, H., Yasukouchi, K., 1982. J. Electroanal. Chem. 140, 187–193.
Tomalia, D.A., Baker, H., Dewald, J.R., Hall, M., Kallos, G., Martin, S., Roeck, J., Ryder, J., Smith, P., 1985. Polym. J. (Tokyo) 17, 117–132.
Tomalia, D.A., Baker, H., Dewald, J.R., Hall, M., Kallos, G., Martin, S., Roeck, J., Ryder, J., Smith, P., 1986. Macromolecules 19, 2466–2468.
Vishnuvardhan, V., Kala, R., Rao, T.P., 2008. Anal. Chim. Acta 623, 53–58.
Wael, K.D., Buschop, H., Smet, L.D., Adriaens, A., 2008. Talanta 76, 309–313.
Wang, G., Xu, J., Chen, H., 2002a. Electrochem. Commun. 4, 506–509.
Wang, J.X., Shi, Z.J., Shi, Z.J., 2002b. Anal. Chem. 74, 1993–1997.
Wu, Q., Storrier, G.D., Parients, F., Wang, Y., Shapleigh, J.P., Abruña, H.D., 1997. Anal. Chem. 69, 4856–4863.
Xiang, C., Zou, Y., Sun, L., Xu, F., 2008. Electrochem. Commun. 10, 38–41.
Yamazaki, I., Araiso, T., Hayashi, Y., Yamada, H., Makino, R., 1978. Adv. Biophys. 11, 249–281.
Yang, W., Bai, Y., Li, Y., Sun, C., 2005. Anal. Bioanal. Chem. 382, 44–50.
Zeng, Y., Huang, Y., Jiang, J., Zhang, X., Tang, C., Shen, G., Yu, R., 2007. Electrochem. Commun. 9, 185–190.
Zhang, L., 2008. Biosens. Bioelectron. 23, 1610–1615.
Zhang, L., Zhang, J., Zhang, C., 2009. Biosens. Bioelectron. 24, 2085–2090.
Zhao, G., Xu, J., Chen, H., 2006. Anal. Biochem. 350, 145–150.
Zhao, G., Yin, Z., Zhang, L., Wei, X., 2005. Electrochem. Commun. 7, 256–260.
Zhou, Y., Zhi, J., Zou, Y., Zhang, W., Lee, S.T., 2008. Anal. Chem. 80, 4141–4146.
Zhu, L., Wang, K., Lu, T., Xing, W., Li, J., Yang, X., 2008. J. Mol. Catal. B 55, 93–98.